Imaging of Apoptosis (Programmed Cell Death) with ^{99m}Tc Annexin V

Francis G. Blankenberg, Peter D. Katsikis, Jonathan F. Tait, R. Eric Davis, Louis Naumovski, Katsuichi Ohtsuki, Susan Kopiwoda, Michael J. Abrams and H.W. Strauss

Departments of Radiology, Genetics, Pathology and Pediatrics (Hematology/Oncology), Stanford University School of Medicine, Stanford, California; Department of Laboratory Medicine, University of Washington, Seattle, Washington; and Anor MED, Inc., Langley, British Columbia, Canada

Apoptosis (programmed cell death) is a critical element in normal physiology and in many disease processes. Phosphatidylserine (PS), one component of cell membrane phospholipids, is normally confined to the inner leaflet of the plasma membrane. Early in the course of apoptosis, this phospholipid is rapidly exposed on the cell's outer surface. Annexin V, an endogenous human protein, has a high affinity for membrane-bound PS. This protein has been labeled with fluorescein and has been used to detect apoptosis in vitro. We describe the use of radiolabeled annexin V to detect apoptosis in vivo. The results are compared to histologic and flow cytometric methods to identify cells and tissues undergoing apoptosis. **Methods:** Annexin V was coupled to hydrazinonicotinamide (HYNIC) and radiolabeled with ^{99m}Tc. Bioreactivity of ^{99m}Tc-HYNIC annexin V was compared with fluorescein isothiocyanate (FITC)-labeled annexin V in cultures of Jurkat T-cell lymphoblasts and in ex vivo thymic cell suspensions undergoing apoptosis in response to different stimuli. In addition, the uptake of FITC annexin V and ^{99m}Tc-HYNIC annexin V was studied in heat-treated necrotic Jurkat T-cell cultures. In vivo localization of annexin V was studied in Balb/c mice injected with ^{99m}Tc-HYNIC annexin V before and after induction of Fas-mediated hepatocyte apoptosis with intravenously administered antiFas antibody. **Results:** Membrane-bound radiolabeled annexin V activity linearly correlated to total fluorescence as observed by FITC annexin V flow cytometry in Jurkat T-cell cultures induced to undergo apoptosis in response to growth factor deprivation ($N = 10$, $r^2 = 0.987$), antiFas antibody ($N = 8$, $r^2 = 0.836$) and doxorubicin ($N = 10$, $r^2 = 0.804$); and in ex vivo experiments on thymic cell suspensions with dexamethasone-induced apoptosis from Balb/c mice ($N = 6$, $r^2 = 0.989$). Necrotic Jurkat T-cell cultures also demonstrated marked increases in radiopharmaceutical (4000–5000-fold) above control values. AntiFas antibody-treated Balb/c mice ($N = 6$) demonstrated a three-fold rise in hepatic uptake of annexin V ($P < 0.0005$) above control ($N = 10$), identified both by imaging and scintillation well counting. The increase in hepatic uptake in antiFas antibody-treated mice correlated to histologic evidence of fulminant hepatic apoptosis. **Conclusion:** These data suggest that ^{99m}Tc-HYNIC annexin V can be used to image apoptotic and necrotic cell death in vivo.

Key Words: annexin V; apoptosis; ^{99m}Tc; hydrazinonicotinamide

J Nucl Med 1999; 40:184–191

Received Jan. 16, 1998; revision accepted May 4, 1998.

For correspondence or reprints contact: Francis G. Blankenberg, MD, Department of Radiology (Pediatric Radiology), Stanford University School of Medicine, 300 Pasteur Dr., Stanford, CA 94305.

Cell death can occur in a disorganized nonphysiologic fashion (necrosis) or in a carefully orchestrated sequence (apoptosis) that leaves little, if any, residue (*1–3*). Necrosis can be caused by mechanical, thermal, electrical or noxious chemical injury and by profound hypoxia, ischemia or respiratory poisons such as cyanide. Cells dying in a necrotic fashion have irreversible membrane failure with resultant cell swelling and chromatin flocculation. The uncontrolled release of a variety of intracellular substances such as hydrogen peroxide, proteases, lipases and deoxyribonucleic (DNA)-ases from necrotic cells can damage adjacent healthy cells and extracellular matrices, resulting in scar and tissue deformity at the site of injury (*3*).

Cell death can also be initiated by several physiologic stimuli that trigger a preprogrammed cellular set of processes resulting in an orderly self-destruction of the cell, apoptotic cell death (*4–6*). Once initiated, the apoptotic sequence results in the self-destruction of a cell. The products of apoptosis are small packets of membrane-bound autodigested cytoplasm and DNA, called apoptotic bodies, which can be easily absorbed by neighboring cells or phagocytes without damage to adjacent tissue or extracellular matrix (*6*). The result is the "physiologic" removal of unwanted superfluous, senescent or damaged cells from the body.

Programmed cell death plays an important role in embryogenesis, regulation of the immune system and homeostasis (*1–6*). Abnormal induction or inhibition of apoptosis has been described in autoimmune and neurodegenerative diseases, cardiomyopathy, myocarditis, cerebral and myocardial ischemia, infectious diseases, cancer development and tumor response to treatment, viral or toxin-induced hepatitis, and organ and bone-marrow transplant rejection (*6*).

Apoptosis was originally described by Kerr et al. (*7*) in 1972, based on examination of tissue specimens from the adrenal glands. DNA fragmentation, a hallmark of apoptosis, occurs relatively late in the process (*8*). Improved immunohistochemical techniques have permitted the identification of apoptosis in situ by specific labeling of nuclear DNA fragmentation (*9*). Recently, several studies identified changes in membrane lipid expression as earlier markers of

apoptosis (*8,10–17*). Designing a technique to image programmed cell death in vivo requires identification of a unique marker that occurs during the process, preferably expressed early after the initiation of the apoptotic cascade. Initial events in the apoptotic cascade include: (a) the activation of cysteine proteases such as interleukin 1 (IL-1)-converting enzyme (ICE) (*5*); (b) activation of sphingomyelinases resulting in production of ceramide, an important signal for several protein kinases; and (c) the exposure of phosphatidylserine (PS) on the cell surface (*8,10,18*). These events occur before the characteristic morphologic changes of plasma membrane blebbing, vesicle formation and cytoskeletal disruption with subsequent cytoplasmic contraction (*4–6*) followed by nuclear chromatin condensation and DNA fragmentation into 200 base pair fragments (DNA ladder formation).

The expression of PS was chosen as the target process to identify apoptotic cells. PS is a simple anionic phospholipid that is normally restricted to the inner leaflet of the plasma membrane. At least two adenosine triphosphate-energy dependent enzyme systems, floppase and translocase (*18,19*) maintain PS in the inner leaflet of the cell membrane. The redistribution of PS from the inner to the outer leaflet of the plasma membrane during apoptosis is believed to be the result of inactivation of floppase and translocase and the activation of a third enzyme, scramblase (*18*). The externalization of PS has been found to be a general feature of apoptosis, occurring before membrane bleb formation and DNA degradation (*8*). Although there is no absolute marker that will always distinguish apoptosis from necrosis, since rapid loss of membrane integrity permits PS on the inner leaflet of the cell membrane access to the extracellular environment, such damage is rare in vivo.

Annexin V, a human protein with a molecular weight of 36 kd, has a high affinity (K_d = 7 nmol) for cell membranes with bound PS (*19*). In vitro assays have been developed that use annexin V to detect apoptosis in hematopoietic cells, neurons, fibroblasts, endothelial cells, smooth muscle cells, carcinomas, lymphomas, all murine embryonic cell types and plant and insect cells (*11,12,17*). Annexin V has also been suggested as an imaging agent to detect thrombi in vivo, because activated platelets express large amounts of PS on their surfaces (*20*). This study describes experiments to test the feasibility of using annexin V to image apoptosis in vivo.

MATERIALS AND METHODS

Preparation of Radiolabeled Annexin V

Human annexin V was produced by expression in *Escherichia coli* as previously described (*21–34*). This material retains PS binding activity equivalent to that of native annexin V (*23*). Human annexin V was conjugated with hydrazinonicotinamide (HYNIC), using methods previously described by Abrams et al. (*24*) and Blankenberg et al. (25).

Concentrations of annexin V were determined using E_{280} = 0.6 mL/mg/cm and molecular weight taken as 35,806 (*21–23*). HYNIC-derivatized annexin V was produced by the gentle mixing of 5.6 mg/mL of annexin V in 20 mmol HEPES, pH 7.4, 100 mmol NaCl for 3 h, shielded from light with succinimidyl 6-HYNIC (Anor MED Inc., Langley, British Columbia) [222 μg in 18.5 μL (42 mmol) solution of N, N-dimethyl formamide] at room temperature. The reaction was quenched with 500 μL of 500-mmol glycine in phosphate-buffered saline (PBS), pH 7.4, and then dialyzed at 4°C against 20 mmol sodium citrate, pH 5.2, 100 mmol NaCl overnight. Precipitate was then removed by centrifuge at 15,000*g* for 10 min. One hundred microliter (100 μg) aliquots of HYNIC annexin V were stored at −70°C. Incorporation of HYNIC into annexin V was determined according to the methods of King et al. (*26*). Protein (0.315 mg in 100 μL of buffer consisting of 20 mmol sodium citrate, pH 5.2, 100 mmol NaCl) was added to 900 μL of a buffer containing 50 mmol sodium acetate, pH 4.73, 100 mmol NaCl, 2.5% (v/v) acetonitrile. Sigma nitrobenzaldehyde (437 nmol in 6.6 μL N,N-dimethyl formamide) was then added, and the reaction incubated for 4.5 h at room temperature. The absorbance was 385 nmol, determined against appropriate reagent blanks. The concentration of HYNIC was determined using $E_{385} = 2.53 \times 10^4$ mol/cm (*24*). Protein concentration was determined colorimetrically with the biscinchonic acid assay kit (Pierce Chemical Company, Rockford, IL) using bovine serum albumin as standard. Incorporation of HYNIC into annexin V was found to be 0.9 mol per mol of annexin V. Membrane-binding activity of HYNIC annexin V and decayed ^{99m}Tc-HYNIC annexin V was determined by a modified competition assay in which 5 nmol/L fluorescein isothiocyanate (FITC; Molecular Probes, Eugene, OR) annexin V was substituted for ^{125}I annexin V (*22,28*). After 15 min at room temperature, the sample was centrifuged, the FITC annexin V bound to the pelleted cells was released with ethylenediaminetetraacetic acid (EDTA) and the released FITC annexin V was measured by fluorometry. In this assay system, unmodified annexin V, HYNIC annexin V and decayed ^{99m}Tc-HYNIC annexin V inhibited 50% of the binding of FITC annexin V at concentrations of 8, 10.5 and 12.3 nmol/L, respectively.

Ten microcuries of ^{99m}Tc-glucoheptonate (DuPont, Wilmington, DE) in 100 μL was incubated with a 100 μL (100 μg of protein) aliquot of HYNIC-derivatized annexin V at room temperature for 1 h, protected from light according to the methods described by Abrams et al. (*24*). After incubation the volume of reaction mixture was brought up to 1 mL with PBS, pH 7.4, with 0.1% human serum albumin (HSA) and collected in 1-mL fractions eluted from a Sephadex G-25 column (Pharmacia, Piscataway, NJ) prerinsed with PBS/0.1% HSA. There was at least a 56% recovery of radiolabeled annexin V after column fractionation with at least 97% radio-purity as seen by instant thin-layer chromatography (ITLC), using PBS as a solvent. Specific activity was >50 μCi/μg protein.

Cell Culture Technique

Jurkat T-cell acute lymphoblastic cultures were grown in RPMI 1640 medium (Applied Scientific, South San Francisco, CA), supplemented with 10% (v/v) fetal calf serum and 290 μg/mL L-glutamine, 100 U/mL penicillin and 100 μg/mL streptomycin. Cells were maintained in the logarithmic growth phase at a concentration of 1–5 × 10^5 cells/mL at 37° C in a 5% CO_2 air incubator under sterile conditions (*27*).

Flow Cytometry Using FITC-Labeled Annexin V

Recombinant annexin V was labeled with FITC purified to yield a fraction containing a single mole of fluorescein per mole of

protein and quantitated by absorbance at 494 nmol, as previously described (*22,28*). Samples were stained (1×10^6 cells per sample) with 5 μg/mL (in deficient RPMI 1640 with 3% fetal calf serum) FITC-labeled annexin V or 5 μg/mL ^{99m}Tc-HYNIC annexin V (10–20 μCi per sample). Cells were incubated on ice for 15 min, washed twice with RPMI 1640, and samples for flow cytometry were fixed with 0.5% paraformaldehyde. Fixed cells were analyzed with a FACStar Plus flow cytometer (Becton Dickinson, Mountain View, CA) within 6 h of FITC-annexin V labeling as previously described (*27*). Radiolabeled cell samples were assayed in a well scintillation counter after completion of the labeling procedure outlined above.

Scintillation Counting

Cell and tissue samples were analyzed with a Packard Cobra II gamma counter (Packard Co., Meriden, CT). The energy window was set at a lower level of 120 keV and an upper level of 170 keV for ^{99m}Tc. When ^{125}I was counted, samples were allowed to decay for at least 24 h. The samples were then recounted using both the technetium window and an ^{125}I setting with a lower level of 20 keV and an upper level of 50 keV. Samples were corrected for any residual down-scatter from technetium.

Ex Vivo Analysis of Apoptotic Murine Thymic Glands

Three- to four-week-old Balb/c mice were injected intraperitoneally with 10 mg/kg dexamethasone. Eight hours after dexamethasone injection, the mice were killed, and single cell suspensions of 1×10^6 thymocytes were prepared by mechanical separation with repeated gentle aspiration and flushing with warmed RPMI 1640 media supplemented with 5% fetal calf serum through sterile 12-mL syringe. Samples were then labeled with FITC annexin V and radiolabeled annexin V and analyzed in the same manner as Jurkat T-cell cultures prepared for flow cytometry and well scintillation counting.

Autoradiography of Renal Tissue

Adult Sprague-Dawley rats (n = 5) were killed 1 h after intravenous administration of 10 mCi ^{99m}Tc-HYNIC annexin V. Macroautoradiographs of tracer distribution in the kidney were recorded from 40 μm frozen coronal sections of renal tissue using single-emulsion Min-R ASA 2000 mammographic film (Kodak Co., Rochester, NY), exposed for 2 h in a Min-R2 mammographic cassette (Kodak). Exposed film was then developed in a Kodak RP X-Omat Processor, Model M6B.

Radionuclide Imaging

A Technicare 420 mobile camera (Technicare, Solon, OH), equipped with a 5-mm pinhole collimator was used to record the radionuclide distribution in mice (*29*). Data were recorded using a 20% window centered on the 140 keV photopeak of technetium into a 128×128 matrix of a dedicated computer system for digital display and analysis (ICON; Siemens Co., Hoffman Estates, IL). All images were recorded for a preset time of 15 min. The percentage of total body counts (% TBC) as seen by region-of-interest image analysis were calculated for the liver and kidneys from images taken 1 h after injection of radiopharmaceutical in the prone anterior projection.

Murine Model of Fas-Mediated Fulminant Hepatitis

Hepatic apoptosis can be induced by intravenous (IV) injection of antiFas antibody. When the antibody binds to the Fas receptors, which are normally expressed on the surface of hepatocytes, apoptosis is initiated (*30*). ^{99m}Tc-HYNIC annexin V was injected after administration of antiFas antibody to determine whether tracer localization increased in an organ undergoing apoptosis in vivo. Four- to five-week-old Balb/c mice were injected intravenously with purified hamster monoclonal antiFas antibody (Jo2, 10 μg per animal; Pharmingen, San Diego, CA) according to the methods described by Ogasawara et al. (30). Two hours later mice were injected intravenously with 0.5–1.5 μg/kg ^{99m}Tc-HYNIC annexin V (20–100 μCi/animal). Subgroups of control and treated mice were co-injected with 0.6 μCi (25 mg) ^{125}I-labeled HSA (Mallinckrodt Inc., St. Louis, MO) iodinated using previously described methods (*31*). Animals were imaged and killed 1 h after administration of radiopharmaceutical, followed by organ removal for well scintillation counting of radioactivity. The livers were paraffin embedded after fixation and decay of activity in formalin. Five-micrometer sections were then stained with hematoxylin and eosin and examined for apoptotic hepatocytes using standard histopathologic criteria (*32*).

Control studies with ^{99m}Tc-labeled HSA were also performed in untreated and antiFas treated mice. The animals were injected with 100–150 μCi ^{99m}Tc-labeled HSA (Amersham, Newark, NJ) (25 mg per animal) and imaged at 2 h, similar to the mice receiving ^{99m}Tc-HYNIC annexin V.

RESULTS

In Vitro Characteristics of Radiolabeled ^{99m}Tc-HYNIC Annexin V

In these experiments the in vitro bioreactivity of radiolabeled-annexin V was compared with FITC-labeled annexin V, which has an affinity for PS nearly identical to native (unlabeled) protein (*20,21*). Cultures of Jurkat T-cell lymphoblasts were induced to undergo apoptosis in response to serum deprivation. In these cultures, the percentage of FITC-labeled annexin V-positive cells and their total fluorescence determined by flow cytometry directly correlated with the uptake of ^{99m}Tc-HYNIC annexin V (Fig. 1). The uptake of ^{99m}Tc-HYNIC annexin V also was correlated linearly with total fluorescence in Jurkat T-cells undergoing apoptosis in response to doxorubicin (0, 25, 50, 75, 100, 125, 150 and 200 ng/mL for 48 h; $r^2 = 0.804$, n = 8) or CH11 antiFas murine monoclonal antibody (Pharmingen) (0, 0.8, 1.6, 3.1, 12.5 and 25 ng/mL for 24 h; $r^2 = 0.836$, N = 6). The maximal increase in ^{99m}Tc HYNIC uptake in doxorubicin and CH11 antiFas antibody-treated cultures compared to control was 25-fold and 500-fold, respectively. When necrosis was induced in Jurkat T-cells by heating cultures at 60°C for 10 and 30 min, there were also marked increases in radiopharmaceutical uptake above control values of 4420% and 5150% (n = 4), respectively. Analysis of thymic tissue removed from dexamethasone-treated mice showed a 635% increase in the percentage of FITC annexin V-positive thymocytes compared to control [51.2% ± 3.2% (n = 3) versus 6.97 ± 0.54 (n = 3), respectively]. Radiolabeled-annexin V uptake was 235% higher in dexamethasone-treated thymocytes compared to control. There was a direct correlation between the percentage of FITC annexin V-

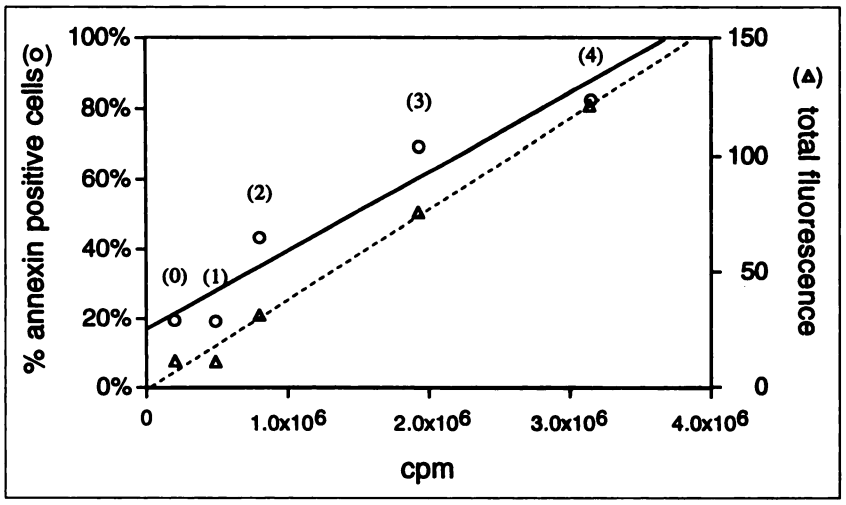

FIGURE 1. Correlation of Tc-HYNIC annexin V binding with flow cytometry. Jurkat T-cell lymphoblast cultures underwent serum deprivation for 0, 1, 2, 3 and 4 d, number of days shown in parentheses. Percentages of FITC annexin-positive cells (0) and total fluorescence (△) determined by flow cytometry are plotted against radioactivity bound to duplicate cell samples expressed as counts per minute (cpm). Best fit lines by linear regression analysis are shown as (—) and (- - -) for % annexin-positive cells (r^2 = 0.922) and total fluorescence (r^2 = 0.987), respectively.

positive thymocytes and the activity of bound ^{99m}Tc-HYNIC annexin V (r^2 = 0.989, n = 6).

Biodistribution of ^{99m}Tc-HYNIC Annexin V

One hour after injection, residual of blood activity was about 3% of the injected dose (ID) (Table 1). The highest concentration (52% of the ID) was found in the kidneys; the organ with the next highest concentration was the liver with 12.8% of the ID. The brain, heart and thymus had the lowest uptakes of radiolabeled-annexin V (less than 0.2% of the ID).

Localization in the kidneys was primarily to the renal cortex (Fig. 2). Other organs that concentrated annexin V were the spleen, liver, stomach and lungs, with activities of 17%, 15.2%, 5.4% and 2.6% ID/gram, respectively. Blood activity was 1.93% ID/gram, which was significantly higher ($P < 0.05$; 2-tailed Student t test) than carcass, muscle or fat (1.13, 0.72 and 1.0% ID/gram, respectively).

TABLE 1
Biodistribution of ^{99m}Tc-HYNIC Annexin V in Untreated Balb/c Mice (n = 10)

	% ID/organ	% ID/g
Brain	0.056% ± 0.08%	0.14% ± 0.21%
Thymus	0.078% ± 0.021%	0.57% ± 0.18%
Lung	0.550% ± 0.170%	2.66% ± 1.01%
Heart	0.160% ± 0.041%	1.57% ± 0.62%
Liver	12.8% ± 2.40%	15.2% ± 6.35%
Spleen	1.68% ± 0.50%	17.0% ± 7.90%
Stomach	1.37% ± 0.38%	5.4% ± 1.80%
Gastrointestinal tract	2.93% ± 0.44%	1.7% ± 0.44%
Kidney	52.0% ± 6.60%	187% ± 31.1%
Muscle	NA	0.72% ± 0.22%
Fat	NA	1.0% ± 0.57%
Carcass	11.7% ± 1.11%	1.13% ± 0.31%
Blood	3.08% ± 1.42%*	1.93% ± 0.89%

*Estimated total blood volume 8.0% of total body weight.

Biodistribution of ^{99m}Tc-HYNIC annexin V 1 h after tail vein injection of 20–50 μCi of radiopharmaceutical (0.5–1.0 μg/kg of protein).

Results expressed as average ± SEM.

%ID = percentage injected dose; NA = not applicable.

Biodistribution of ^{99m}Tc-HYNIC Annexin V During Fas-Mediated Hepatic Apoptosis

Biodistribution assays were performed on control and antiFas antibody-treated mice 1 h after injection of 20–50 μCi ^{99m}Tc-HYNIC annexin V. The hepatic uptake of ^{99m}Tc-HYNIC annexin V rose from 12.8% ± 2.40% ID (n = 10) in controls to 52.0% ± 10.8% ID (n = 6) in treated mice ($P < 0.0005$) 2 h after antiFas antibody injection (Fig. 3). Renal uptake fell 60.5% below control values after antiFas antibody treatment. There was <5% excretion of administered radiopharmaceutical into the urine in control or treated animals. Carcass activity fell by 38% 2 h after administration of antiFas antibody. The uptake of radiolabeled annexin V of other organs or tissue did not significantly change after antiFas treatment.

Liver sections from mice treated with antiFas antibody showed a spectrum of nuclear changes characteristic of

FIGURE 2. ^{99m}Tc-HYNIC annexin V autoradiograph of renal tissue. Note marked uptake of ^{99m}Tc-HYNIC annexin is virtually limited to renal cortex with minimal activity in medullary and papillary regions.

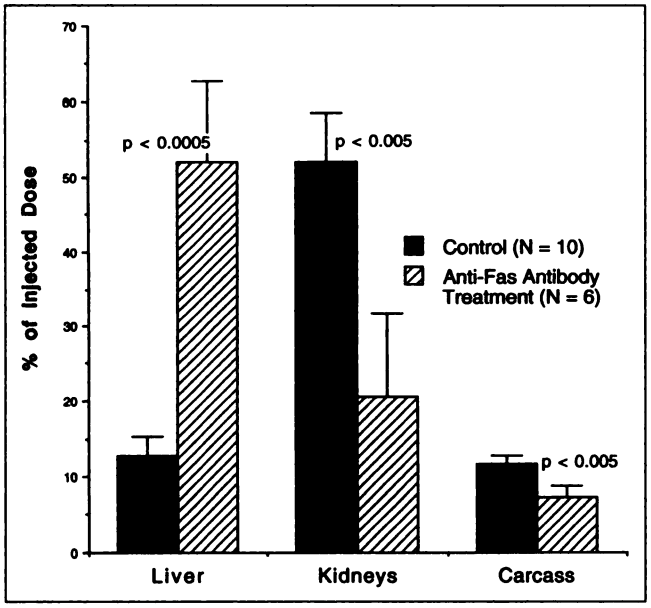

FIGURE 3. Biodistribution of Tc^{99m}-HYNIC annexin V after antiFas antibody treatment. Mean values of activities of liver, kidneys, and carcass expressed as percentage of injected dose ± SEM are shown. *P* values are shown for 2-tailed student *t* test comparing treated and control groups. N = number of animals in each group.

apoptosis (margination of chromatin, pyknosis and karyorrhexis), with focally associated hemorrhage (peliosis) 2 h after treatment (Fig. 4).

Subgroups of mice were co-injected with ^{125}I-labeled HSA to control nonspecific uptake of inert protein from the circulation (Table 2). Hepatic uptake was 168% above control values at 2 h after antiFas antibody injection, whereas renal activity increased 73%. The uptake of ^{125}I-HSA in the carcass or other sampled organs did not change significantly with antiFas treatment.

Imaging of Fas-Mediated Hepatic Apoptosis with ^{99m}Tc-HYNIC Annexin V

One hour after injection of 100 μCi ^{99m}Tc-HYNIC annexin, images in control animals demonstrated a high concentration of radiolabeled annexin V in the kidneys, with a general distribution in other organs (Fig. 5A). The liver was not visualized as a separate structure. In mice treated with antiFas antibody, there was a diffuse, marked increase in hepatic uptake of ^{99m}Tc-HYNIC annexin V. The fall in renal activity found in the biodistribution studies was readily visualized with external imaging after antiFas treatment.

Control studies were recorded using a nonspecific protein, ^{99m}Tc-labeled HSA (100 μCi, 25 mg protein) in untreated and antiFas-treated mice. There was no perceptible change in liver or renal activity in the ^{99m}Tc-HSA images of treated mice compared to controls (Fig. 5B).

DISCUSSION

These data demonstrate that radiolabeled annexin V can be used to quantify apoptotic cells in culture and in cell suspension and that it concentrates sufficiently in tissue undergoing apoptosis in vivo to permit external imaging. Localization in necrotic cells is probably due to either binding to PS on the inner plasma membrane leaflet of cells with irreversible membrane damage or failure of energy-dependent cellular systems to restrict PS to the inner leaflet, thereby allowing the passive redistribution of PS from the inner to outer leaflet of the plasma membrane. These in vitro findings suggest that radiolabeled annexin V may be able to directly quantify apoptosis or necrotic cell death in vivo. These results parallel work by van den Eijnde et al. (16), which supports the use of annexin V for in situ detection of apoptotic cells after intracardiac injection of biotin-labeled annexin V in developing embryos using immunohistochemical techniques.

Administration of ^{99m}Tc-HYNIC annexin V to mice with Fas-mediated fulminant liver injury demonstrated a marked increase in the hepatic localization of the tracer, which correlated with histologic evidence of apoptosis. The increase of ^{125}I-HSA hepatic uptake after antibody treatment (less than half of the rise in ^{99m}Tc-HYNIC annexin V uptake) was most likely due to an expanded extracellular fluid

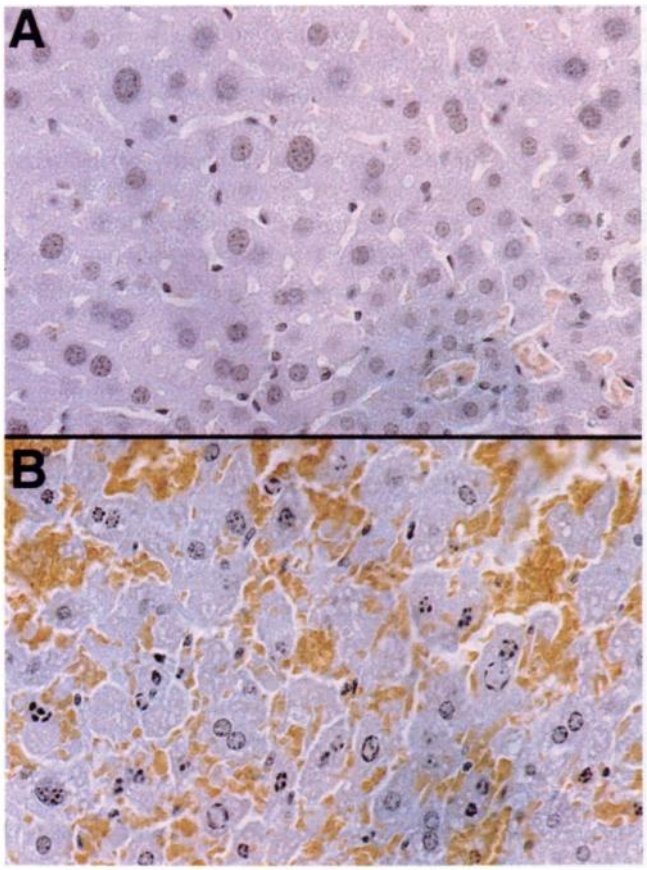

FIGURE 4. Histologic sections of mouse liver after antiFas antibody treatment. (A) H&E-stained histologic section from a control (untreated) mouse shows hepatocytes with normal hexagonal morphology. (B) Two hours after antiFas treatment there is extensive apoptotic nuclear change with dense peripheral nuclear chromatin condensation, slight cytoplasmic retraction and interstitial hemorrhage.

TABLE 2
Biodistribution of ^{125}I-HSA After Anti-Fas Treatment

	% ID/organ	
	Controls (n = 4)	2-h anti-Fas (n = 5)
Liver	4.66 ± 1.34	12.5 ± 3.34 ($P < 0.01$)
Kidneys	1.60 ± 0.44	2.76 ± 0.58 ($P < 0.025$)
Carcass	43.1 ± 6.59	37.4 ± 7.56 (NS)
	Organ weight (g)	
Liver	1.02 ± 0.11	1.22 ± 0.11 ($P < 0.05$)
Kidneys	0.30 ± 0.03	0.32 ± 0.026 (NS)
Carcass	12.7 ± 0.39	12.5 ± 0.90 (NS)

Results are expressed as the mean ± SEM of the percentage of injected dose per organ (% ID/organ). *P* values for two-tailed Student *t* tests for significance of anti-Fas treated mice compared with control group shown in parentheses.
NS = not significant ($P > 0.05$).

volume from the breakdown of hepatic endothelial cells as described by Lacronique et al. (*32*). This was confirmed by a 20% increase in hepatic weight with treatment. In theory, the disruption of the vasculature in this Fas-mediated model of acute apoptosis could have increased annexin V localization to the liver because of secondary localization on activated platelets. Immunohistochemical staining of hepatic specimens with rabbit antihuman annexin V IgG polyclonal antibody in other studies revealed peripheral hepatocyte staining only, with no localization in the vasculature or at sites of hemorrhage (*25*). In addition, the relatively rapid clearance of annexin V from the blood makes it unlikely that marked localization would occur at sites of reduced perfusion in the absence of specific binding. Previous studies demonstrated marked decrease in hepatic radiocolloid localization in the presence of marked inflammation of the liver (*33*). These observations suggest that the majority of increased liver localization in the Fas antibody-treated animals was due to specific annexin V localization in apoptotic hepatocytes.

The high cortical concentration of annexin V in the kidney may relate to the unique phospholipid composition of the renal cortex, which has higher amounts of PS compared to the papillary regions (*34*). Another possibility is the nonspecific uptake of low-molecular-weight proteins such as annexin V by the proximal renal tubule cells noted in studies of peptides and antibody fragments (*35,36*). After treatment with antiFas antibody, the distribution of ^{99m}Tc-HYNIC annexin V changed markedly from controls, with the majority of radiolabeled annexin V localizing to the liver in treated mice. This was probably a result of the marked increase in the number of annexin binding sites expressed by the apoptotic liver. It is unlikely that equilibrium binding effects due to differences in the affinity of binding sites in the kidney and carcass versus apoptotic liver could have a major impact on biodistribution, because the serum half-life of intravenously administered annexin V is only 3–7 min (*20*). The renal uptake of ^{125}I-HSA was increased in treated mice compared to controls. This was in marked contrast to the decrease in annexin V uptake in treated mice compared to controls. A shift of fluid from the intracellular to extracellular renal compartment may explain the increase in kidney uptake of ^{125}I-HSA without a change in weight.

The Fas receptor/ligand system has been shown to be crucial in the regulation of the immune system, autoimmune disorders and homeostasis and/or stress conditions in extralymphoid tissues in a variety of apparently unrelated conditions, such as antitumor processes (*5*), host defense against infection, immunologic or toxic injuries, viral hepatitis and organ and bone marrow transplant rejection (*6*). Injection of antiFas antibody (equivalent of Fas ligand), which binds to hepatic Fas receptors (antigen), leads to massive apoptosis of hepatocytes and death of animals within a few hours (*30, 32*), mimicking the sequence of pathological changes seen in acute liver failure secondary to hepatitis caused by viruses or toxins in humans.

Radiolabeled-annexin V imaging of Fas-mediated apopto-

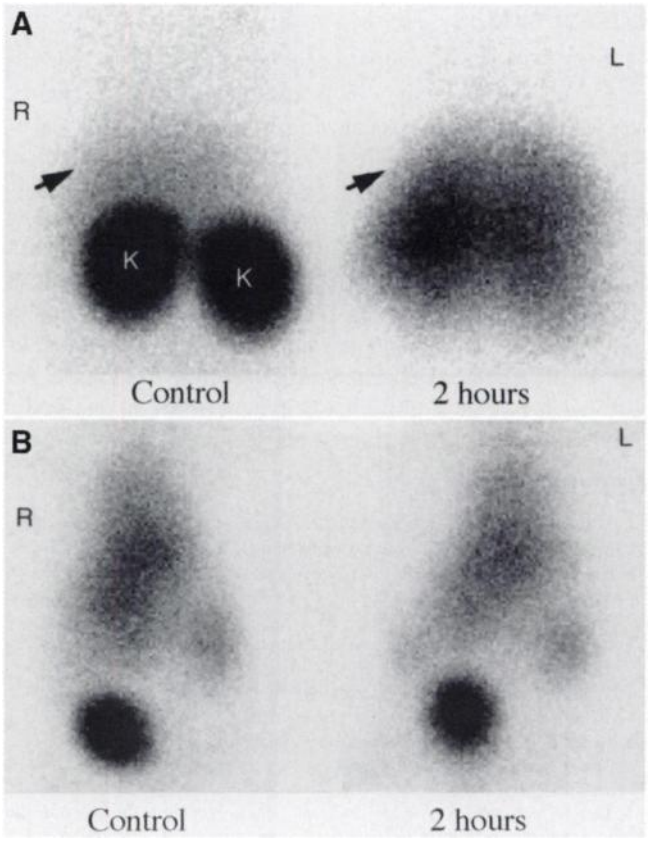

FIGURE 5. Imaging Fas-mediated fulminant hepatic apoptosis with radiolabeled annexin V. (A) Representative control and antiFas antibody treated (2 h) mice are shown after injection of ^{99m}Tc-HYNIC annexin V. Liver activity (shown by arrow) was markedly higher in antiFas antibody-treated mice (46.5% TBC) compared to controls (8.08% TBC). Kidney activity (K) fell from 61.6% TBC to 15.0% TBC 2 h after antiFas treatment (R = right. L = left). (B) Representative control and antiFas antibody treated mice after injection of ^{99m}T-HSA. Bladder activity was photographed in panel B animals.

sis therefore has broader applications other than the monitoring of toxin- or virally induced hepatitis. Acute liver, heart, lung, renal transplant rejection and graft versus host disease (in bone marrow transplant recipients) are mediated by activated T-lymphocytes that are alloreactive in organ transplant recipients and autoreactive in bone marrow transplant patients (*6*). Recent data suggest that cytolytic T-lymphocytes induce target cell death primarily by Fas-mediated apoptosis in these disorders (*37–40*). Additional studies also suggest that chronic transplant rejection in both organ and bone transplant recipients is due to the induction of Fas-mediated endothelial cell apoptosis and proliferation (*41, 42*). Preliminary data from our laboratory suggest that ^{99m}Tc-HYNIC annexin V can be used to image acute cardiac transplant rejection (*43*). Although our initial in vivo studies demonstrate the feasibility of radiolabeled-annexin V imaging, we have not demonstrated that apoptosis in all types of tissue can be visualized. In addition, the number of cells that must be in the process of apoptosis for visualization with radiolabeled annexin V is yet to be determined.

CONCLUSION

^{99m}Tc-HYNIC annexin V appears to be a useful agent to image sites of apoptotic cell death in vivo. In vitro studies suggest that it will also localize in areas of necrosis.

ACKNOWLEDGMENTS

This work was supported in part by the Child Health Research Fund, Lucile Packard Children's Hospital at Stanford University, by the National Institutes of Health grant no. HL-47151 and by funds from the Division of Nuclear Medicine, Department of Radiology, Stanford. We also thank Bonnie Bell for her help in performing this study.

REFERENCES

1. Lennon SV, Martin SJ, Cotter TG. Dose-dependent induction of apoptosis in human tumor cell lines by widely diverging stimuli. *Cell Prolif.* 1991;24:203–214.
2. Tepper CG, Studzinski GP. Resistance of mitochondrial DNA to degradation characterizes the apoptotic but not the necrotic mode of human leukemia cell death. *J Cell Biochem.* 1993;52:352–361.
3. Darzynkiewicz Z. Apoptosis in antitumor strategies: modulation of cell cycle or differentiation. *J Cell Biochem.* 1995;58:151–159.
4. Steller H. Mechanisms and genes of cellular suicide. *Science.* 1995;267:1445–1449.
5. Nagata S, Golstein P. The Fas death factor. *Science.* 1995;267:1449–1456.
6. Thompson BC. Apoptosis in the pathogenesis and treatment of disease. *Science.* 1995;267:1456–1462.
7. Kerr JF, Wyllie AH, Currie AR. Apoptosis: a basic biological phenomenon with wide-ranging implications in tissue kinetics. *Br J Cancer.* 1972;26:239–257.
8. Martin SJ, Reutelingsperger CPM, McGahon AJ. Early redistribution of plasma membrane phosphatidylserine is a general feature of apoptosis regardless of the initiating stimulus: inhibition by overexpression of Bcl-2 and Abl. *J Exp Med.* 1995;182:1545–1556.
9. Gavrieli Y, Sherman Y, Ben-Sasson S. Identification of programmed cell death in situ via specific labeling of nuclear DNA fragmentation. *J Cell Biol.* 1992;119:493–501.
10. Koopman G, Reutelingsperger CPM, Kuijten GAM, Keehnen RMJ, Pals ST, van Oers MHJ. Annexin V for flow cytometric detection of phosphatidylserine expression on B cells undergoing apoptosis. *Blood.* 1994;84:1415–1420.
11. Boersma AWM, Kees N, Oostrum RG, Stoter G. Quantification of apoptotic cells with fluorescein isothiocynate-labeled annexin V in Chinese hamster ovary cell cultures treated with cisplatin. *Cytometry.* 1996;24:123–130.
12. O'Brien IEW, Reutelingsperger CPM, Holdaway KM. Annexin V and TUNEL use in monitoring the progression of apoptosis in plants. *Cytometry.* 1997;29:28–33.
13. van Engeland M, Nieland LJW, Ramaekers FCS, Schutte B, Reutelingsperger CPM. Annexin V-affinity assay: a review on an apoptosis detection system based on phosphatidylserine exposure. *Cytometry.* 1998;31:1–9.
14. Allen RT, Hunter III WJ, Agrawal DK. Morphological and biochemistry characterization and analysis of apoptosis. *J Pharmacol Toxicol Methods.* 1997;37:215–228.
15. Vermes I, Haanen C, Steffens-Nakken H, Reutelingsperger CPM. A novel assay for apoptosis flow cytometry detection of phosphatidylserine expression on early apoptotic cells using fluorescein labelled annexin V. *J Immunol Methods.* 1995;184:39–51.
16. van den Eijnde SM, Luijsterburg AJM, Boshart L, et al. In situ detection of apoptosis during embryogenesis with annexin V: from whole mount to ultrastructure. *Cytometry.* 1997;29:313–320.
17. Reutelingsperger CPM, van Heerde WL. Annexin V, the regulator of phosphatidylserine-catalyzed inflammation and coagulation during apoptosis. *Cell Mol Life Sci.* 1997;53:527–532.
18. Zwaal RFA, Schroit AJ. Pathophysiologic implications of membrane phospholipid asymmetry in blood cells. *Blood.* 1997;89:1121–1132.
19. van Heerde WL, de Groot PG, Reutelingsperger CPM. The complexity of the phospholipid binding protein annexin V. *Thromb and Haemost.* 1995;73:172–179.
20. Stratton JR, Dewhurst TA, Kasina S, et al. Selective uptake of radiolabeled annexin V on acute porcine left atrial thrombi. *Circulation.* 1995;92:3113–3121.
21. Wood BL, Gibson DF, Tait JF. Increased phosphatidylserine exposure in sickle cell disease: flow-cytometric measurement and clinical associations. *Blood.* 1996;88:1873–1880.
22. Tait JF, Engelhardt S, Smith C, Fujikawa K. Prourokinase-annexin V chimeras: construction, expression, and characterization of recombinant proteins. *J Biol Chem.* 1995;270:21594–21599.
23. Tait JF, Smith C. Site-specific mutagenesis of annexin V: role of residues from Arg-200 to Lys-207 in phospholipid binding. *Arch Biochem Biophys.* 1991;288:141–144.
24. Abrams MJ, Juweid M, tenKate CI. Technetium-99m-human polyclonal IgG radiolabeled via the hydrazino nicotinamide derivative for imaging focal sites of infection in rats. *J Nucl Med.* 1990;31:2022–2028.
25. Blankenberg FG, Katsikis PD, Tait JF, et al. In vivo detection and imaging of phosphatidylserine expression during programmed cell death. *Proc Natl Acad Sci USA.* 1998;95:6349–6354.
26. King TP, Zhao SW, Lam T. Preparation of protein conjugates via intermolecular hydrazone linkage. *Biochemistry.* 1986;25:5774–5779.
27. Blankenberg FG, Katsikis PD, Storrs RW, et al. Quantitative analysis of apoptotic cell death using proton nuclear magnetic resonance spectroscopy. *Blood.* 1997;89:3778–3786.
28. Tait JF, Gibson D. Measurements of membrane phospholipid asymmetry in normal and sickle-cell erthyrocytes by means of annexin V binding. *J Lab Clin Med.* 1994;123:741–748.
29. Pieri P, Fischman AJ, Ahmad M, Moore RH, Callahan RJ, Strauss HW. Cardiac blood pool scintigraphy in rats and hamsters: comparison of five radiopharmaceuticals and three pin-hole collimator apertures. *J Nucl Med.* 1991;32:851–855.
30. Ogasawara J, Watanabe-Fukunaga R, Adachi M. Lethal effects of the anti-Fas antibody in mice. *Nature.* 1993;364:806–809.
31. Tait JF, Cerqueira MD, Dewhurst TA. Evaluation of annexin V as a platelet-directed thrombus targeting agent. *Thromb Res.* 1994; 75:491–501.
32. Lacronique V, Mignon A, Fabre M. Bcl-2 protects from lethal hepatic apoptosis induced by an anti-Fas antibody in mice. *Nature Med.* 1996;2:80–86.
33. Mettler FA, Guiberteau MJ. In: Mettler FA Jr, Guiberteau MJ, eds. *Essentials of Nuclear Medicine Imaging*, 2nd ed. Philadelphia, PA: WB Saunders; 1985:206–246.
34. Sterin-Speziale N, Kahane VL, Setton CP, del Carmen Fernandez M, Speziale EH. Compartmental study of rat renal phospholipid metabolism. *Lipids.* 1992;27:10–14.
35. Kobayashi H, Yoo TM, Sim IS, et al. L-lysine effectively blocks renal uptake of ^{125}I or Tc-labeled anti-Tac disulfide-stabilized Fr fragment. *Cancer Res.* 1996;56:3788–3795.
36. Lang L, Jagoda E, Wu CH. Factors influencing the in vivo pharmacokinetics of peptides and antibody fragments: the pharmacokinetics of two PET-labeled low molecular weight proteins. *Q J Nuc Med.* 1997;41:53–61.

37. Seino K, Kayagaki N, Bashuda H, Okumura K, Yagita H. Contribution of Fas ligand to cardiac allograft rejection. *Int Immunol.* 1996;8:1347–1354.
38. Laguens RP, Cabeza Meckert PM, San Martino J, Perrone S, Favaloro R. Identification of programmed cell death (apoptosis) in situ by means of specific labeling of nuclear DNA fragments in heart biopsy samples during acute rejection episodes. *J Heart Lung Transplant.* 1996;15:911–918.
39. Jollow KC, Sundstrom JB, Gravanis MB, Kanter K, Herskowitz A, Ansari AA. Apoptosis of mononuclear cell infiltrates in cardiac allograft biopsy specimens questions studies of biopsy-cultured cells. *Transplantation.* 1997;63:1482–1489.
40. Matiba B, Mariani SM, Krammer PH. The CD95 System and the death of a lymphocyte. *Immunology.* 1997;9:59–68.
41. Bergese SD, Klenotic SM, Wakely ME, Sedmak DD, Orosz CG. Apoptosis in murine cardiac grafts. *Transplantation.* 1997;63:320–325.
42. Dong C, Wilson JE, Winters GL, McManus BM. Human transplant coronary artery disease: pathologic evidence for fas-mediated apoptotic cytotoxicity in allograft arteriopathy. *Lab Invest.* 1996;74:921–931.
43. Vriens PW, Blankenberg FG, Davis ER, et al. In vivo imaging of apoptosis during cardiac allograft rejection using radiolabeled annexin V [Abstract]. *J Thorac Cardiovasc Surg.* 1998: in press.